BIOCHEMISTRY
including biophysical chemistry & molecular biology

Article

pubs.acs.org/biochemistry

Effects of Tryptophan Content and Backbone Spacing on the Uptake Efficiency of Cell-Penetrating Peptides

Hanna A. Rydberg, Maria Matson, Helene L. Åmand, Elin K. Esbjörner, and Bengt Nordén*

Department of Chemical and Biological Engineering/Physical Chemistry, Chalmers University of Technology, Kemivägen 10, S-412 96 Gothenburg, Sweden

Supporting Information

ABSTRACT: Cell-penetrating peptides (CPPs) are able to traverse cellular membranes and deliver macromolecular cargo. Uptake occurs through both endocytotic and nonendocytotic pathways, but the molecular requirements for efficient internalization are not fully understood. Here we investigate how the presence of tryptophans and their position within an oligoarginine influence uptake mechanism and efficiency. Flow cytometry and confocal fluorescence imaging are used to estimate uptake efficiency, intracellular distribution and toxicity in Chinese hamster ovarian cells. Further, membrane leakage and lipid membrane affinity are investigated. The peptides contain eight arginine residues and one to four tryptophans, the tryptophans positioned either at the N-terminus, in the middle, or evenly distributed along the amino acid sequence. Our data show that the intracellular distribution varies among peptides with different tryptophan content and backbone spacing. Uptake efficiency is higher for the peptides with four tryptophans in the middle, or evenly distributed along the peptide sequence, than for the peptide with four tryptophans at the N-terminus. All peptides display low cytotoxicity except for the one with four tryptophans at the N-terminus, which was moderately toxic. This finding is consistent with their inability to induce efficient leakage of dye from lipid vesicles. All peptides have comparable affinities for lipid vesicles, showing that lipid binding is not a decisive parameter for uptake. Our results indicate that tryptophan content and backbone spacing can affect both the CPP uptake efficiency and the CPP uptake mechanism. The low cytotoxicity of these peptides and the possibilities of tuning their uptake mechanism are interesting from a therapeutic point of view.

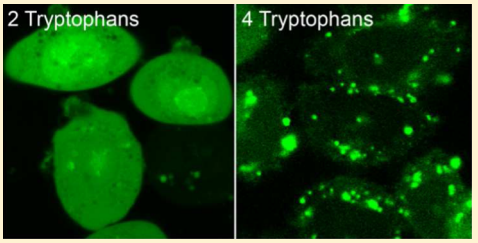

Advances in molecular and cellular biology have resulted in new drug targets such as siRNA and different types of therapeutic proteins. A common feature of these drug leads is that they target intracellular sites. Hence, a main obstacle is to transport the bulky and/or charged biomacromolecules across the cell membrane to their intracellular targets, which requires efficient and nontoxic cellular internalization. Various vectors have been developed for the delivery of macromolecular therapeutics,[1,2] among which the cell-penetrating peptides (CPPs) stand out as promising candidates because of their intrinsically rapid and highly efficient internalization, and their typically low toxicities.[3]

CPPs have been reported to cross cellular membranes by in principle two different routes: by endocytotic pathways or by nonendocytotic, energy-independent direct membrane penetration (transduction) mechanisms.[4,5] Whereas endocytosis is the predominant pathway for many CPPs, some sequences (e.g., those rich in arginines) appear to be able to use both routes in parallel.[6−8] However, reported results diverge, and the exact uptake mechanisms or partitioning between different pathways appear to depend on both peptide sequence and concentration and seem also to be affected by the nature of the attached cargo and possibly also on cell type or even on cell culture conditions.[9,10] This has sometimes led to confusing or contradicting conclusions complicating attempts to design optimal CPP sequences. Despite the advantage of peptide-based delivery vectors being relatively easy to modify with respect to chemical properties via variation of the amino acid composition, few studies have explored systematically how patterning of amino acid sequence affects CPP properties.

CPPs commonly have a high content of positively charged residues, e.g., arginines and lysines. The chemical nature of these positive charges may drastically influence cellular uptake and membrane interactions.[7,11−14] Our group discovered that a penetratin variant in which all lysine residues were substituted with arginines had better internalization efficiency than penetratin itself.[11,12] As a result of these findings in addition to the discovery of the efficiently translocated arginine-rich domain of Tat and the development of the oligoarginine sequence,[15−17] much of the CPP research has been focused on the functions of pure oligoarginines. Longer polyarginine chains indeed generally result in more efficient uptake,[6,18,19] but the majority of reports suggest optimal lengths in the range from 8 to 15 arginines.[6,15,19] Octaarginines (R_8) are commonly used as CPPs as they are sufficiently long to provide high cellular uptake[9] but still short enough to be easy and cost-effective to prepare. In addition, Rothbard et al.[18] showed that not only the number but also the spacing of arginine residues can influence

Received: April 10, 2012
Revised: June 15, 2012
Published: June 19, 2012

   dx.doi.org/10.1021/bi300454k | *Biochemistry* 2012, 51, 5531−5539

uptake by introducing aminocaproic acid as a backbone spacer into a heptaarginine.

The oligoarginine sequence has also been developed in other ways, e.g., by the introduction of a tryptophan at the C-terminus of a heptaarginine.[7,20] Maiolo et al.[21] have shown that uptake of R_7W is in fact better than that of R_7 alone. Tryptophan is a hydrophobic amino acid, but because of its aromaticity, it also has a strong preference for interactions at the membrane interface[22] and has important anchoring functions in most membrane proteins.[23−25] The exact role of tryptophans in CPPs is less clear and has mainly been studied in the context of penetratin where contradictory results have been reported. As an example, a tryptophan to phenylalanine substitution has been reported to decrease the rate of cellular uptake or to have no apparent effect at all.[7,26,27] These findings made us interested in how the number and distribution of tryptophans in a sequence may influence CPP function.

We here explore how uptake and intracellular localization as well as cytotoxicity of oligoarginine-inspired CPPs may be tuned by introduction of one or several tryptophan residues into the sequence. We specifically address the extent to which the exact primary sequence influences CPP function. For this purpose, we designed six CPPs all containing eight arginines but with different numbers and sequence positions of tryptophans. We investigate how the number of tryptophans may influence the uptake by comparing octaarginines with one, two, three, or four tryptophans attached to the N-terminus. To investigate the role of the exact primary sequence, we compared the W_4R_8 peptide to two other peptides with the same amino acid content, but with the tryptophans placed either as a block in the middle of the sequence or distributed evenly along the sequence (Table 1). We have found that our designed CPPs can enter cells either by endocytotic, by nonendocytotic pathways, or by both. Because nonendocytotic entry may be associated with cytotoxicity, we also examined their toxicity to cells as well as their ability to induce lipid vesicle leakage and their affinity for lipid vesicle membranes. Our data show that the uptake efficiency indeed increases with increased tryptophan content, but also that uptake is more efficient if the tryptophan residues are placed as a block in the middle of the sequence or distributed evenly along the sequence than if they are placed as a block at the N-terminus.

Table 1. Peptide Sequences

peptide	sequence[a]
WR_8	**W**RRRRRRRR
W_2R_8	**WW**RRRRRRRR
W_3R_8	**WWW**RRRRRRRR
W_4R_8	**WWWW**RRRRRRRR
RWR	RRRR**WWW**RRRR
RWmix	R**W**RR**W**RR**W**RR**W**R

[a]Tryptophans are bold.

EXPERIMENTAL PROCEDURES

Materials. Peptides (>95% purity) were purchased from Innovagen (Lund, Sweden) or Alta Bioscience (Birmingham, U.K.). The fluorescent marker, 5-FAM (5-carboxyfluorescein), was conjugated to the N-terminus via an Ahx linkage. The N-termini of the nonlabeled peptides were acetylated. All C-termini were amidated. 1-Palmitoyl-2-oleoyl-*sn*-glycero-3-phosphocholine (POPC) and 1-palmitoyl-2-oleoyl-*sn*-glycero-3-phosphoglycerol (POPG) were from Larodan Fine Chemicals (Malmö, Sweden), and 1,2-distearoyl-*sn*-glycero-3-phosphoethanolamine-*N*-[poly(ethylene glycol) 2000] (DSPE-MPEG) was from BioTrend (Köln, Germany). 7-Aminoactinomycin D (7-AAD) and LysoTracker Red DND-99 were from Invitrogen (Stockholm, Sweden). A Guava Nexin kit (Millipore, Solna, Sweden) was used for toxicity measurements.

Cell Culture. Chinese hamster ovary cells (CHO-K1) were cultured in Ham's F12 medium supplemented with 10% fetal bovine serum and L-glutamine (2 mM) in a humidified atmosphere containing 5% CO_2 at 37 °C. For confocal microscopy analysis, cells were seeded in glass bottom culture dishes at a density of 17000 cells/cm^2 and cultured for 48 h prior to experiment. For analysis on the Guava flow cytometer, cells were seeded in 96-well plates at a density of 7000 cells/well in 200 μL of growth medium and cultured for 48 h prior to experiment.

Confocal Laser Scanning Microscopy. The cells were washed once with Ham's F12 and then incubated with 5 μM 5-FAM-labeled peptide diluted in serum free Ham's F12 medium for 1 h at either 37 or 4 °C. For experiments performed at 4 °C, the medium was supplemented with 10 mM HEPES to obtain CO_2-independent medium for incubation outside the incubator. A confocal laser scanning microscopy system (Leica TCS SP, Wetzlar) equipped with 488 nm Ar and 543 nm He/Ne lasers and a HCX PL APO CS 63 × 1.32 oil immersion objective was used for acquisition of confocal fluorescence images. 5-FAM-labeled peptides were excited at 488 nm, and emission was recorded between 500 and 550 nm. 7-AAD (1 μM) was added immediately before confocal analysis to stain nuclei of dead cells. 7-AAD was excited at 543 nm, and emission was measured at 640−700 nm. To examine potential colocalization between peptide and acidic compartments, 50 nM LysoTracker Red was added to the cell culture at the same time as the 5-FAM-labeled peptides. Cells were imaged after incubation for 1 h at 37 °C. LysoTracker Red was excited at 543 nm, and emission was recorded between 590 and 710 nm.

Quantification of Cellular Uptake. Cellular uptake was quantified using a Millipore Guava 8HT (Millipore) flow cytometer. The cells were washed with Ham's F12 medium and then treated with 5-FAM-labeled peptide (0.5−10 μM) and dissolved in serum free Ham's F12 medium for 1 h at 37 °C. The cells were washed twice with a 20 mM HEPES/150 mM NaCl mixture (pH 7.4) in the first wash supplemented with heparin (100 μg/mL) to sequester extracellular and externally bound peptide.[28] The cells were detached by trypsin treatment (10 min), which also aids digestion of any remaining externally bound peptide. Analysis of cellular uptake was performed using Millipore Guava Incyte software. The cells were gated using forward/side scatter, to measure uptake in only live cells. The mean cellular fluorescence (5000 analyzed cells per sample) was plotted as a function of peptide concentration.

Measurement of Peptide Toxicity. Cell toxicity was measured on a Millipore Guava 8HT flow cytometer using two different methods. First, the number of dead cells after incubation with 5 or 10 μM unlabeled peptide for 1, 2, and 3 h was measured by just prior to measurement adding 1 μM 7-AAD, which is a cell-impermeable DNA stain that detects dead cells. As a negative control, cells incubated with Ham's F12 medium only were used, and as a positive control, cells were incubated with ethanol (final concentration of ∼15%) for 15 min. Second, cells were stained with reagents with a Millipore Guava Nexin assay kit according to the manufacturer's

dx.doi.org/10.1021/bi300454k | *Biochemistry* 2012, 51, 5531−5539

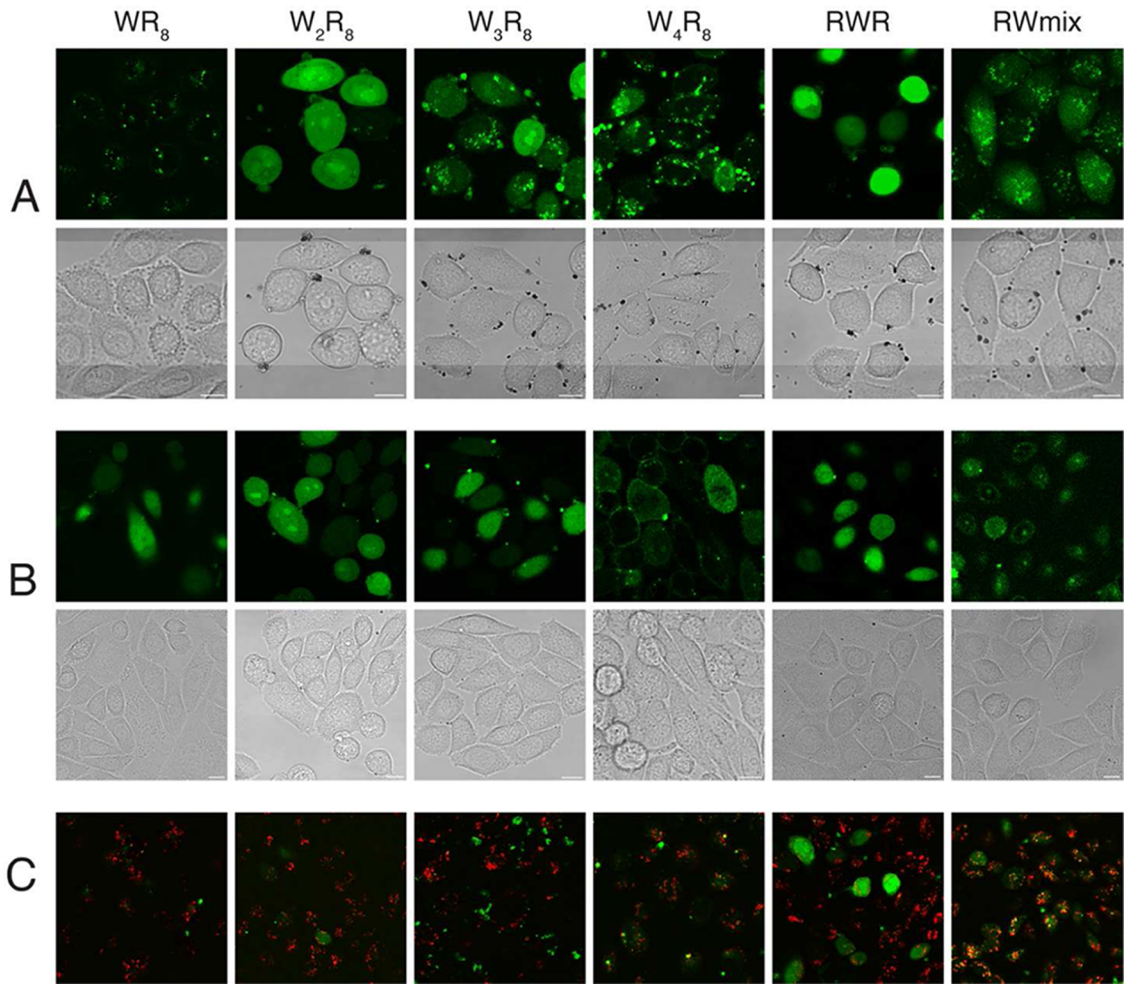

Figure 1. Confocal imaging of live cells incubated with 5 μM 5-FAM-labeled peptides for 1 h at 37 °C (A) and 4 °C (B) and at 37 °C with LysoTracker Red (C), showing intracellular localization. In panels A and B, the peptides are visualized in green above the transmission images. All scale bars are 10 μm. In panel C, merged images are shown for colocalization between the peptide and LysoTracker Red. The cells were washed prior to imaging. The laser intensity and photomultiplier settings have been adjusted to yield the best visualization of each image, and the intensities are thus not directly comparable.

instructions. This assay contains Annexin-V PE (Annexin-V conjugated with Phycoerythrin), which binds to phosphatidylserine lipids that are presented at the outer leaflet of the plasma membrane in an early stage of apoptosis, and 7-AAD (as above). Cells were incubated with 5 or 10 μM unlabeled peptide for 1 h at 37 °C. Cells incubated in Ham's F12 medium only and cells incubated with 1 μM staurosporin, for 3 h at 37 °C, were used as negative and positive controls, respectively. The fraction of cells positive for Annexin-V PE but negative for 7-AAD was determined.

In Vitro Membrane Leakage. Large unilamellar lipid vesicles (liposomes) were prepared by extrusion.[29] A POPC/POPG solution (80/20 molar ratio) dissolved in chloroform was mixed in a round bottom flask. The solvent was evaporated under reduced pressure using a rotary evaporator, and the remaining lipid film was placed under vacuum for 2 h to remove any traces of solvent. Vesicles were formed by dispersion of the lipid film in a 50 mM carboxyfluorescein/HEPES solution under vortexing (5 min), followed by six freeze−thaw cycles (liquid nitrogen to 50 °C) and extrusion 21 times through Nucleopore polycarbonate filters with a pore diameter of 100 nm using an extruder (LiposoFast-Pneumatic, Avestin). The liposomes were separated from nonencapsulated material by gel filtration on a Sephadex G-50 column (GE Healthcare) and eluted in HEPES buffer [10 mM HEPES, 107 mM NaCl, and 1 mM EDTA (pH 7.4)] prepared to match the osmolarity of the carboxyfluorescein buffer, thereby preventing leakage effects caused by osmotic pressure.[29] Liposomes were diluted in buffer to a final lipid concentration of 25 μM. Peptides were added at peptide/lipid ratios of 0.04 and 0.08. The bee venom peptide melittin was used as a positive control, but because of its potency, at a significantly lower peptide/lipid ratio (0.004). Leakage was monitored as a function of time by measuring the increase in fluorescence of dequenched dye using a Spex Fluorolog τ-3 spectrofluorometer (Jobin Yvon Horiba). Carboxyfluorescein was excited at 490 nm, and the emission intensity was recorded at 520 nm. Complete leakage was obtained by adding Triton-X to a final concentration of 0.1 vol % at the end of each experiment. The percentage of leakage was calculated according to eq 1:

$$\text{leakage}\,(\%) = [I(t) - I_0]/(I_{\text{Triton X-100}} - I_0) \times 100 \qquad (1)$$

where I_0 and $I_{\text{Triton X-100}}$ are the average of 10 succeeding data points taken prior to addition of peptide and after complete leakage induction by Triton X-100, respectively.

dx.doi.org/10.1021/bi300454k | *Biochemistry* 2012, 51, 5531−5539

Affinity of the Peptide for Lipid Membrane Vesicles. Tryptophan fluorescence was used to monitor the binding of the peptide to lipid vesicles, as its intrinsic emission shows both a blue shift and an increase in quantum yield when a peptide is transferred into a less polar environment.[30] POPC, POPG, and DSPE-MPEG lipids, dissolved in chloroform, were mixed at a molar ratio of 16/3/1. DSPE-MPEG was added to reduce peptide-induced vesicle aggregation occurring at high peptide/lipid ratios. The liposomes were produced as described above, but the lipid film was dispersed in HEPES buffer [10 mM HEPES, 100 mM NaCl, and 1 mM EDTA (pH 7.4)]. The vesicles were extruded 21 times through two polycarbonate filters with a pore size of 100 nm using a hand-held syringe extruder (Avestin); 50 μL of peptide (100 μM) was added to 3000 μL of HEPES buffer, and the tryptophan emission was monitored using a Spex Fluorolog τ-3 spectrofluorometer (Jobin Yvon Horiba). Samples were excited at 280 nm, and fluorescence spectra were recorded between 315 and 400 nm. The samples were thereafter titrated with lipid vesicles (1 μL aliquots of a 10 mM stock solution), and a spectrum was recorded for each step in the titration. Because it is known that cationic peptides have a tendency to adsorb to quartz, we modified the surface of the cuvette walls with 1% (w/v) polyethylenimine as previously described, and mixing was carefully performed three times by plunging a custom-made metallic cuvette mixer to minimize peptide adsorption.[30] The fractions of free and bound peptide were calculated from each spectrum in the titration series by projection onto reference spectra recorded on free and bound peptide, respectively, and the apparent binding constant and the number of lipids in a binding site, K_{app} and n, respectively, were calculated as described in the Supporting Information.

RESULTS

Uptake and Intracellular Localization of a Peptide. To explore how incorporation of tryptophan residues into an octaarginine sequence may influence uptake and intracellular localization of the CPP and to then further explore how the tryptophan/arginine sequence patterns influence CPP properties, we first investigated their interaction with and internalization into live CHO-K1 cells using confocal laser scanning microscopy. Figure 1 shows the intracellular distribution of the six peptides [WR_8, W_2R_8, W_3R_8, W_4R_8, RWR, and RWmix (see Table 1)] following a 1 h incubation at 37 or 4 °C. The staining pattern varies substantially among the different peptides. We observe punctuate staining for WR_8, W_3R_8, W_4R_8, and RWmix at 37 °C, showing that the internalized peptide is, at least in part, confined to intracellular vesicles. This suggests that endocytosis contributes to peptide internalization. WR_8 shows mainly punctuate staining, whereas W_3R_8, W_4R_8, and RWmix in addition show diffuse staining throughout the cytoplasm in a majority of the cells. For W_4R_8, the punctuate staining is mostly localized close to the plasma membrane or in the cytosol but clearly excluded from the nucleus. W_2R_8 and RWR display both weak punctuate uptake and diffuse homogeneous staining throughout the cytoplasm and interestingly also stronger intensity in cellular structures that are morphologically identified as the cell nucleus and nucleoli. The diffuse intracellular staining indicates either direct membrane transduction or efficient escape from endocytotic vesicles and is seen in most cells for RWR and in ~20% of the cells for W_2R_8. None or very few cells (approximately two to five cells per dish) were positive for 7-AAD at 37 °C (data not shown), indicating that the peptides are not highly toxic.

To examine whether uptake into the cytoplasm occurs directly through plasma membrane transduction or via endosomal escape, we performed the same experiment described above at 4 °C to eliminate contributions from endocytosis. Figure 1B shows that uptake occurs at 4 °C, with diffuse staining for most of the peptides, but that the punctuate staining is absent. Especially W_4R_8 shows very low levels of uptake at 4 °C, with very little intracellular staining but with evident localization of the peptide at the cell membrane, indicating that its main route of internalization is via endocytosis. WR_8 shows, in contrast to the punctuate staining seen at 37 °C, weak staining of the cytoplasm in a minority of the cells, whereas the remaining peptides give much clearer staining of the cytoplasm, and to some extent also the nucleus. Nuclear staining with W_2R_8 and RWR is similar to what was observed at 37 °C, suggesting that trafficking to the nucleus follows direct membrane transduction. No cells were stained with 7-AAD (data not shown).

To further investigate the mechanisms of uptake of six peptides into cells, colocalization between peptide and acidic compartments (late endosomes and lysosomes) was monitored, using LysoTracker Red DND-99. Colocalization was seen for RWmix (Figure 1C), which suggests that this peptide is internalized via endocytosis and thereafter transported to lysosomal compartments. The other peptides do not colocalize significantly with vesicles in the late endosomal–lysosomal system.

Quantification of Cellular Uptake. While the confocal imaging experiments show uptake and intracellular localization of peptides, it is not feasible to extract quantitative information regarding the amount of internalized peptide from statistical analysis of confocal images. To obtain a quantitative measure of their efficiency, we instead used flow cytometry to determine the relative amounts of internalized peptide after incubation for 1 h. Figure 2 shows the mean cellular fluorescence as a function

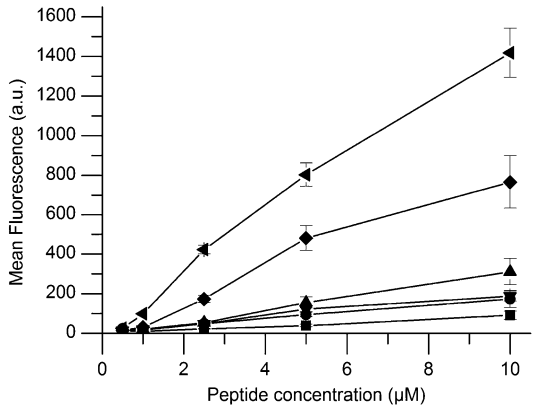

Figure 2. Cellular uptake of 5-FAM-labeled peptides in live CHO-K1 cells after incubation for 1 h at 37 °C. The highest uptake intensity is seen for RWmix (leftward-pointing triangle), followed by, in order of decreasing intensity, RWR (◆), W_3R_8 (▲), W_4R_8 (▼), W_2R_8 (●), and WR_8 (■). The uptake is measured as the mean cellular fluorescence from flow cytometric analysis of all live cells positive for the fluorophore. The background level (mean cellular fluorescence for untreated cells) is 10–15 au, which means that the values for both 0.5 and 1 μM are hard to detect. Error bars are standard errors of the mean (n = 6).

dx.doi.org/10.1021/bi300454k | *Biochemistry* 2012, 51, 5531–5539

of peptide concentration. The mean cellular fluorescence increases with increasing concentration for all tested peptides, and the effect is relatively linear in the tested concentration regime. There is an increase in fluorescence intensity for peptides with increasing tryptophan content up to three tryptophans at the N-terminus of the peptide. The W_4R_8 peptide interestingly shows lower levels of intracellular fluorescence than W_3R_8. The main differences are observed upon comparison of the three peptides that contain four tryptophans and eight arginines (W_4R_8, RWR, and RWmix). The RWR peptide has considerably higher intracellular fluorescence than W_4R_8, and RWmix displays a fluorescence intensity at 10 μM almost 10-fold higher than that of W_4R_8, indicating that the distribution of amino acids within the peptide is decisively important for their uptake efficiency.

Cytotoxicity in Cell Culture. For a CPP to be a functional vector, its uptake efficiency must be high and it must be well tolerated and therefore exhibit low levels of cytotoxicity. The absence of 7-AAD staining in the confocal imaging experiments (see above) indicates that the peptides are not acutely toxic or immediately causing necrosis due to membrane leakage. However, to examine toxicity in further detail and to obtain quantitative information, we performed two flow cytometric experiments. As a first approach, the amount of 7-AAD-stained cells after treatment with two different concentrations of peptide for 1−3 h was monitored. Figure 3A shows that WR_8 and W_2R_8 do not induce cell death at levels significantly above the negative control (Ham's F12 medium). For the peptides with three and four tryptophans, a slight increase in the number of dead cells is seen, both with an increasing peptide concentration and with an increasing incubation time. Especially W_4R_8 shows a conspicuous time-dependent increase in toxicity, with >20% dead cells, ∼4 times higher than the values seen for the other two peptides containing four tryptophans, after incubation for 3 h.

As a next approach, even if the number of dead cells was relatively low for all peptides except W_4R_8, we wanted to explore whether the peptides induce apoptosis. We used an apoptosis kit based on Annexin-V and 7-AAD to stain cells with surface-exposed phosphatidylserine and/or with permeabilized membranes. Annexin-V, which binds to externalized phosphatidylserine, is a marker of early apoptosis, whereas 7-AAD stains the nuclei of cells with permeabilized membranes, i.e., late apoptotic cells and necrotic cells. In Figure 3B, the percentages of cells positive for Annexin-V but negative for 7-AAD are presented, identifying only the fraction of early apoptotic cells. The results show that the peptides cause relatively low levels of early apoptosis, not much higher than for the cells treated with Ham's F12 medium only. However, a slight increase in early apoptosis is seen with an increasing amount of tryptophans in the peptide sequence, with a minor difference among the three peptides containing four tryptophans being distinguishable. W_4R_8 and RWmix may be slightly more toxic than RWR, but the difference is not statistically significant.

In Vitro Membrane Leakage. Because it appears that several of our designed CPPs can enter cells via direct membrane penetration mechanisms yet appear not to give rise to acute levels of cytotoxicity associated with membrane leakage, we decided to explore further their interactions with lipid membranes. We measured the leakage of carboxyfluorescein, encapsulated at a self-quenching concentration in lipid vesicles prepared from synthetic lipids, to detect if the peptides have a tendency to disrupt membrane integrity, which would

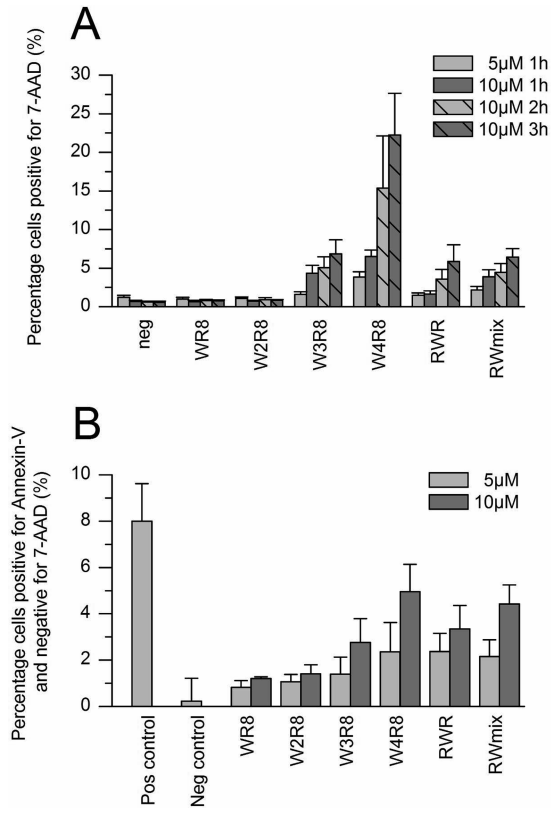

Figure 3. Cytotoxicity measurement showing the percentage of cells positive for 7-AAD and Annexin-V after incubation with 5 and 10 μM unlabeled peptide at 37 °C. (A) Cells positive for 7-AAD are depicted. As a positive control, cells were incubated with 70% ethanol for 15 min rendering 84% cells positive for 7-AAD with a standard deviation of 5.7 (not shown). As a negative control, cells were incubated with Ham's F12 medium. The diagram shows an average of three replicates on three different occasions, with error bars being the standard deviation. After incubation for 1 h, the difference in toxicity between the peptides points at the toxicity being higher for the peptides with three and four tryptophans than for those with one and two tryptophans. However, after incubation for 2 and 3 h with 10 μM peptide, an evident increase in toxicity is seen for peptide W_4R_8. At the same time, WR_8 and W_2R_8 are not more toxic than cell medium. (B) Cells positive for Annexin-V and negative for 7-AAD are depicted. As a positive control, cells were incubated with 1 μM staurosporin for 3 h, and as a negative control, cells were incubated with Ham's F12 medium. The diagram shows an average of two or three replicates on four different occasions, with error bars being the standard error of the mean. The difference between the percentage of cells positive for Annexin-V, thus being in an early apoptotic stage, for the respective peptide is not significant.

result in content leakage. This could occur due to pore formation or related membrane disruptive mechanisms. Figure 4 shows the increase in carboxyfluorescein fluorescence as a result of dequenching of released dye as a function of time after addition of peptide. The experiments were performed at peptide/lipid ratios of 0.04 and 0.08. All peptides give rise to relatively low levels of leakage, but the kinetics are typical of peptide-induced leakage (i.e., with a fast initial component and at least one second slower component). Unspecific leakage usually results in a linear increase in fluorescence and occurs on much longer time scales. Interestingly, RWmix and W_4R_8 give rise to higher leakage levels, consistent with the relative frequencies of early apoptosis but not with the occurrence of dead cells. RWmix and W_4R_8 cause ∼6% leakage, RWR ∼3%,

dx.doi.org/10.1021/bi300454k | *Biochemistry* 2012, 51, 5531−5539

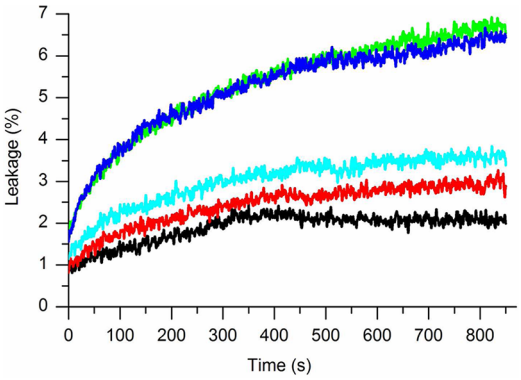

Figure 4. Peptide-induced leakage of carboxyfluorescein from lipid vesicles represented as a percentage compared to complete lysis (100%). The leakage was recorded as a function of time after addition of peptide at a peptide/lipid ratio of 0.08. The highest leakage was seen for W_4R_8 (green) and RWmix (blue), followed by RWR (turquoise), W_3R_8 (red), and W_2R_8 (black).

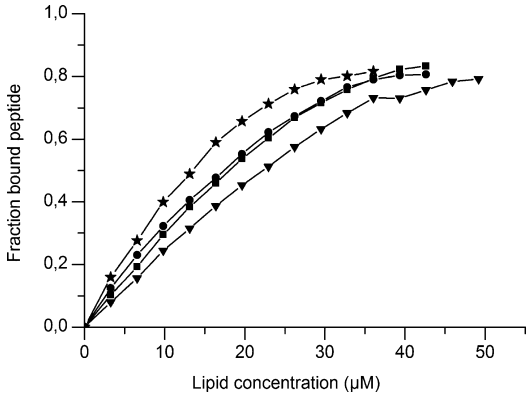

Figure 5. Binding curves for the association of RWR (★), W_4R_8 (◆), W_3R_8 (■), and RWmix (▼) with POPC/POPG/MPEG liposomes. The fraction of bound peptide compared to the nontitrated reference value for maximal binding is shown as a function of lipid concentration.

and W_3R_8 and W_2R_8 ~2% (Table 2). As a comparison, melittin (a strongly lytic peptide) shows as much as 29% leakage, even if added at a 10−20-fold lower peptide/lipid ratio.

Table 2. Leakage Data and Binding Constants[a]

peptide	leakage (%)[b]	leakage (%)[c]	K_{app} ($\times 10^6$ M^{-1})	n
WR_8	–	–	–	–
W_2R_8	2.0	2.1	–	–
W_3R_8	3.2	2.9	10	19
W_4R_8	5.7	6.7	5	16
RWR	3.3	3.6	8	14
RWmix	5.5	6.4	13	24
melittin	29.0	29.0	–	–

[a]Induced leakage of liposomes consisting of an 80/20 POPC/POPG mixture. Peptide/lipid ratios are 0.04 and 0.08 for the RW peptides and 0.004 for melittin. The apparent binding constant and the number of lipids in a binding site for peptides binding to 16/3/1 POPC/POPG/DSPE-PEG vesicles are presented. [b]Ratio of 0.04. [c]Ratio of 0.08.

Affinity of the Peptide for Lipid Membrane Vesicles. Because binding to the cell membrane is likely to be the first step in the internalization of CPPs and because we see a difference between the peptides, with regard to both uptake and toxicity, we wanted to investigate if there is also any discrepancy between the binding affinities of the peptides for lipid membranes. The peptides were titrated with aliquots of liposomes, and the fraction of bound peptide was calculated on the basis of the wavelength shift and intensity change in tryptophan fluorescence. Singular-value decomposition analysis of the recorded tryptophan emission spectra showed that only two components are significant for the system (data not shown), which validate the assumption that there are only two states in the system, free and membrane-bound peptide. In Figure 5, the fraction of bound peptide is plotted versus the total lipid concentration. The magnitude of binding is similar with binding saturation being reached at a peptide/lipid ratio of ~1/25 for the four peptides that could be examined in this assay (W_3R_8, W_4R_8, RWR, and RWmix). For WR_8 and W_2R_8, no reliable results were obtained, which might have been caused by insufficient shifts in tryptophan emission. Further, only minor differences in the steepness of the binding curves are noticed. The slope in the region of half-maximal binding, i.e., at ~15 μM lipid, is almost identical for W_3R_8 and W_4R_8, whereas it is slightly higher for RWR and slightly lower for RWmix. From the fitting of a quadratic equation to the least-squares projection of the bound peptide, the apparent binding constant and the number of lipids in a binding site were calculated. All peptides were shown to have apparent binding constants of the same magnitude (see Table 2) that are comparable to binding constants previously obtained for penetratin (1.5×10^6 M^{-1} for an 80/20 DOPC/DOPG mixture).[30] These results indicate that the specific peptide sequence rather than the binding constant is the crucial factor in these peptides' chemical physical properties.

DISCUSSION

Arginine-rich peptides have been well studied because of their efficient cell internalization properties. They have been characterized in terms of their routes of uptake into cells, their interaction with membranes, and how amino acid spacing influences both of these properties.[11,12,18] However, the impact of introducing other amino acids into an arginine-rich sequence has not been extensively explored. On the basis of the finding that addition of one tryptophan to a heptaarginine increases its uptake efficiency,[21] we wanted to explore systematically how tryptophan content and the distribution of tryptophan within an oligoarginine sequence would affect its CPP properties. We found that increasing tryptophan content has a positive effect on uptake efficiency but that the effect is not trivial as we observe a decrease in efficacy when introducing a fourth tryptophan at the N-terminus of octaarginine. Interestingly, altering the spacing of tryptophans within the oligoarginine sequence has a much stronger effect on uptake efficiency, and we also observed major differences in intracellular distribution. Our results suggest that introduction of tryptophans into arginine-rich peptides can improve uptake and that it might be possible to tailor tryptophan/arginine CPPs with particular sequence patterns to gain control of their subsequent intracellular localization. We will discuss this as well as implications of peptide design for endocytosis and direct translocation mechanisms.

The RWmix sequence has the highest uptake level of the peptides in our study and is up to 10 times as efficient as the corresponding peptide with all tryptophans in a block at the N-

dx.doi.org/10.1021/bi300454k | Biochemistry 2012, 51, 5531−5539

terminus. The even distribution of the tryptophan residues along the extension of the peptide opens up the possibility that it might realize secondary amphipathicity when interacting with the cell surface. The helical wheel projection in Figure 6 shows

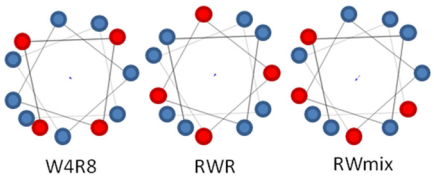

Figure 6. Helical wheel projection of three peptides containing four tryptophans. Arginine residues are colored blue and tryptophan residues red. Membrane Protein Explorer MPEx 3.2 free software from the the S. White laboratory at the University of California (Irvine, CA) was used.

that all tryptophans would assemble on one face of the peptide if it adopts a helical conformation. Takechi et al.[19] have indicated that α-helix-forming polyarginines have greater uptake in cells, and it might also be possible that RWmix adopts an α-helical structure, which could explain the superior uptake.

Having all four tryptophans at the N-terminal end of the peptide sequence, as in W_4R_8, obviously decreases its uptake efficiency compared to those of RWmix and RWR. This amino acid distribution gives the peptide primary amphipathicity with a distinctly charged part and a highly hydrophobic part. Interestingly, W_4R_8 uptake appears to be more dependent on endocytosis than that of the other 12-mer peptides or the shorter versions with two and three tryptophans. In addition, we observed punctuate staining closely localized to the cell membrane (presumably endosomes filled with peptide) at 37 °C. The in vitro experiments with lipid vesicles suggested that this peptide had a strong tendency to aggregate vesicles in solution, and we therefore speculate that this peptide may disturb the process by which endosomes are pinched off from the plasma membrane because of its primary amphipathicity where the tryptophans can anchor the peptide strongly in the lipid membrane and the arginine "tail" may stick out and adhere to other negatively charged cell membrane components. This could also explain its relatively poor uptake.

A comparison of the intracellular localizations for the six peptides at 37 °C, at 4 °C, and with stained late endosomes demonstrates that the uptake routes differ depending on tryptophan content and backbone spacing, with endocytosis having varying levels of importance. We show that several of the designed peptides are able to cross cellular membranes and gain access to the cytosol and even the cell nucleus. This transduction occurs also at 4 °C and can therefore not be considered to be any form of active transport. The RWmix peptide is the only peptide for which colocalization with late endosomes and lysosomal compartments is seen. The other peptides that were internalized via endocytosis may either escape endosomes at an earlier stage, disturb the endosome maturation process, or prevent trafficking to late endosomal compartments.

We found that most of our designed CPPs are relatively nontoxic, which is promising from a therapeutic application perspective, yet we may ask whether high uptake coincides with high toxicity. Interestingly, this does not seem to be the case. When 7-AAD is added to the cells, no, or only very few, cells were stained. The cytotoxicity assays point to toxicity for these peptides being only slightly higher than for cell medium only, except for W_4R_8, which shows a clear increase in cytotoxicity with time, possibly explained by its primary amphipathicity that might induce a disturbance of the endosome maturation process as a result of endosome aggregation or adherence of endosomes to the cell membrane. This higher toxicity for W_4R_8 could possibly also explain its apparent low intracellular uptake because dead cells were excluded in the flow cytometry analysis. In addition, in the early apoptosis assay, a certain variation in toxicity between the peptides is seen, coinciding with the results from the leakage measurement. It might be possible that the low levels of early apoptosis seen could be caused by membrane leakage resulting in depolarization.

Octaarginine does not induce content leakage in liposomes,[31] but it is still possible that an accumulation of tryptophan could be a triggering factor as it introduces hydrophobicity into the peptide sequence. However, oligoarginines can disturb membranes, and the formation of small transient pores, as for Arg9,[32] cannot be ruled out. We show that leakage is substantially lower than for the potent leakage-causing peptide melittin, but we can still discriminate variation between the peptides, with W_4R_8 and RWmix inducing somewhat higher levels of leakage. This together with the higher toxicity monitored for W_4R_8 points to the fact that not only tryptophan content but also tryptophan backbone spacing may influence the degree of toxicity.

The results suggest that the peptides in this study, especially RWmix and RWR, may be efficient vectors for intracellular transport because of their high uptake efficiency and relatively low toxicity in mammalian cells. The uptake efficiency of RWmix is superior to that of RWR and those of all of the other peptides. However, RWmix is to a large extent found in vesicular structures within the cell, whereas RWR exhibits a higher level of uptake into the cytosol and the nucleus. Also, the toxicity of RWR is somewhat lower than for RWmix. These results suggest that CPPs with an accumulation of tryptophans in the middle of the sequence are superior as vectors for transport to the cytosol and the nucleus. Placing the hydrophobic tryptophans at the N-terminus instead impairs the efficiency. It is, however, possible that the cargo, in this case a hydrophobic 5-FAM, will influence the result and that the optimal sequence may need to be adjusted according to the cargo of interest.

Interestingly, our designed peptides also show similarity in sequence to certain types of antimicrobial peptides (AMPs), which may also have a high content of arginines and tryptophans. It has been suggested that these two amino acids can contribute to antimicrobial properties because of the tryptophan's preference for the lipid membrane interfacial region and the arginine's facilitation of peptide−membrane interactions at anionic lipid surfaces through hydrogen bond formation and electrostatic attraction.[33] However, our results suggest that the RW peptides are in fact relatively benign in mammalian cells, which is also in accord with the dual properties recently described for the human antimicrobial peptide LL-37, which has potent activity against bacteria, while behaving like a typical CPP in the vicinity of mammalian cells.[34] Further, it is possible that subtle variation in the amino acid sequence may, as demonstrated here, affect the physicochemical interactions between the peptide and cellular membranes in such a way that uptake efficiency as well as uptake pathways and cytotoxicity will be modulated. Further investigation may

dx.doi.org/10.1021/bi300454k | *Biochemistry* 2012, 51, 5531−5539

thus not only result in the identification of better CPPs or better AMPs but also help to shed light on the fundamental differences and similarities between these two classes of functional membrane-interacting peptides.

CONCLUSIONS

In conclusion, this study importantly indicates that the tryptophan content and backbone spacing of CPPs is a determinant for both uptake efficiency and routes of uptake into CHO-K1 cells. The uptake pattern differs between peptides with different tryptophan contents and compositions, showing both endocytotic and nonendocytotic uptake mechanisms. In addition, several of the peptides that we designed show direct uptake into the cytoplasm in combination with intracellular localization in the nucleus. Interestingly, the uptake efficiency clearly differs between peptides having same amino acid content but with an altered tryptophan distribution. Furthermore, the peptides, with one exception, show high bioavailability, with relatively low levels of cytotoxicity and liposome leakage, making these peptides promising for future applications as vectors for intracellular transport.

ASSOCIATED CONTENT

Supporting Information

Flow cytometry histogram of uptake, plot of gated cells from the Nexin assay, tryptophan emission spectra for binding of the peptide to titrated liposomes, and calculation of binding constants. This material is available free of charge via the Internet at http://pubs.acs.org.

AUTHOR INFORMATION

Corresponding Author

*E-mail: norden@chalmers.se. Phone: +46 (0) 31 772 3041.

Funding

This work was supported by a grant to B.N. from King Abdullah University of Science and Technology (KAUST) and to E.K.E. from the Lennander foundation.

Notes

The authors declare no competing financial interest.

ACKNOWLEDGMENTS

We thank Prof. Per Lincoln for help with MATLAB calculations.

ABBREVIATIONS

CPP, cell-penetrating peptide; AMP, antimicrobial peptide; CD, circular dichroism; SVD, singular-value decomposition; R, arginine; W, tryptophan; 7-AAD, 7-aminoactinomycin D; CHO, Chinese hamster ovary.

REFERENCES

(1) Ziello, J. E., Huang, Y., and Jovin, I. S. (2010) Cellular Endocytosis and Gene Delivery. *Mol. Med. 16*, 222−229.

(2) Guo, J. F., Bourre, L., Soden, D. M., O'Sullivan, G. C., and O'Driscoll, C. (2011) Can non-viral technologies knockdown the barriers to siRNA delivery and achieve the next generation of cancer therapeutics? *Biotechnol. Adv. 29*, 402−417.

(3) Eguchi, A., and Dowdy, S. F. (2009) siRNA delivery using peptide transduction domains. *Trends Pharmacol. Sci. 30*, 341−345.

(4) Schmidt, N., Mishra, A., Lai, G. H., and Wong, G. C. L. (2010) Arginine-rich cell-penetrating peptides. *FEBS Lett. 584*, 1806−1813.

(5) Ter-Avetisyan, G., Tuennemann, G., Nowak, D., Nitschke, M., Herrmann, A., Drab, M., and Cardoso, M. C. (2009) Cell Entry of Arginine-rich Peptides Is Independent of Endocytosis. *J. Biol. Chem. 284*, 3370−3378.

(6) Mitchell, D. J., Kim, D. T., Steinman, L., Fathman, C. G., and Rothbard, J. B. (2000) Polyarginine enters cells more efficiently than other polycationic homopolymers. *J. Pept. Res. 56*, 318−325.

(7) Thorén, P. E. G., Persson, D., Isakson, P., Goksor, M., Onfelt, A., and Nordén, B. (2003) Uptake of analogs of penetratin, Tat(48−60) and oligoarginine in live cells. *Biochem. Biophys. Res. Commun. 307*, 100−107.

(8) Duchardt, F., Fotin-Mleczek, M., Schwarz, H., Fischer, R., and Brock, R. (2007) A comprehensive model for the cellular uptake of cationic cell-penetrating peptides. *Traffic 8*, 848−866.

(9) Wender, P. A., Galliher, W. C., Goun, E. A., Jones, L. R., and Pillow, T. H. (2008) The design of guanidinium-rich transporters and their internalization mechanisms. *Adv. Drug Delivery Rev. 60*, 452−472.

(10) Ziegler, A., and Seelig, J. (2011) Contributions of Glycosaminoglycan Binding and Clustering to the Biological Uptake of the Nonamphipathic Cell-Penetrating Peptide WR(9). *Biochemistry 50*, 4650−4664.

(11) Åmand, H. L., Bostrom, C. L., Lincoln, P., Nordén, B., and Esbjörner, E. K. (2011) Binding of cell-penetrating penetratin peptides to plasma membrane vesicles correlates directly with cellular uptake. *Biochim. Biophys. Acta 1808*, 1860−1867.

(12) Åmand, H. L., Fant, K., Nordén, B., and Esbjörner, E. K. (2008) Stimulated endocytosis in penetratin uptake: Effect of arginine and lysine. *Biochem. Biophys. Res. Commun. 371*, 621−625.

(13) Persson, D., Thorén, P. E. G., Esbjörner, E. K., Goksör, M., Lincoln, P., and Nordén, B. (2004) Vesicle size-dependent translocation of penetratin analogs across lipid membranes. *Biochim. Biophys. Acta 1665*, 142−155.

(14) Walrant, A., Correia, I., Jiao, C. Y., Lequin, O., Bent, E. H., Goasdoue, N., Lacombe, C., Chassaing, G., Sagan, S., and Alves, I. D. (2011) Different membrane behaviour and cellular uptake of three basic arginine-rich peptides. *Biochim. Biophys. Acta 1808*, 382−393.

(15) Futaki, S., Suzuki, T., Ohashi, W., Yagami, T., Tanaka, S., Ueda, K., and Sugiura, Y. (2001) Arginine-rich peptides: An abundant source of membrane-permeable peptides having potential as carriers for intracellular protein delivery. *J. Biol. Chem. 276*, 5836−5840.

(16) Vives, E., Brodin, P., and Lebleu, B. (1997) A truncated HIV-1 Tat protein basic domain rapidly translocates through the plasma membrane and accumulates in the cell nucleus. *J. Biol. Chem. 272*, 16010−16017.

(17) Wender, P. A., Mitchell, D. J., Pattabiraman, K., Pelkey, E. T., Steinman, L., and Rothbard, J. B. (2000) The design, synthesis, and evaluation of molecules that enable or enhance cellular uptake: Peptoid molecular transporters. *Proc. Natl. Acad. Sci. U.S.A. 97*, 13003−13008.

(18) Rothbard, J. B., Kreider, E., Vandeusen, C. L., Wright, L., Wylie, B. L., and Wender, P. A. (2002) Arginine-rich molecular transporters for drug delivery: Role of backbone spacing in cellular uptake. *J. Med. Chem. 45*, 3612−3618.

(19) Takechi, Y., Yoshii, H., Tanaka, M., Kawakami, T., Aimoto, S., and Saito, H. (2011) Physicochemical Mechanism for the Enhanced Ability of Lipid Membrane Penetration of Polyarginine. *Langmuir 27*, 7099−7107.

(20) Thorén, P. E. G., Persson, D., Esbjörner, E. K., Goksor, M., Lincoln, P., and Nordén, B. (2004) Membrane binding and translocation of cell-penetrating peptides. *Biochemistry 43*, 3471−3489.

(21) Maiolo, J. R., Ferrer, M., and Ottinger, E. A. (2005) Effects of cargo molecules on the cellular uptake of arginine-rich cell-penetrating epeptides. *Biochim. Biophys. Acta 1712*, 161−172.

(22) Yau, W. M., Wimley, W. C., Gawrisch, K., and White, S. H. (1998) The preference of tryptophan for membrane interfaces. *Biochemistry 37*, 14713−14718.

(23) Landoltmarticorena, C., Williams, K. A., Deber, C. M., and Reithmeier, R. A. F. (1993) Nonrandom distribution of amino-acids in the transmembrane segments of human type-I single span membrane-proteins. *J. Mol. Biol. 229*, 602−608.

(24) von Heijne, G. (1994) Membrane-proteins: From sequence to structure. *Annu. Rev. Biophys. Biomol. Struct. 23*, 167−192.
(25) Reithmeier, R. A. F. (1995) Characterization and modeling of membrane-proteins using sequence-analysis. *Curr. Opin. Struct. Biol. 5*, 491−500.
(26) Derossi, D., Joliot, A. H., Chassaing, G., and Prochiantz, A. (1994) The 3rd helix of the antennapedia homedomain translocates through biological membranes. *J. Biol. Chem. 269*, 10444−10450.
(27) Christiaens, B., Grooten, J., Reusens, M., Joliot, A., Goethals, M., Vandekerckhove, J., Prochiantz, A., and Rosseneu, M. (2004) Membrane interaction and cellular internalization of penetratin peptides. *Eur. J. Biochem. 271*, 1187−1197.
(28) Kaplan, I. M., Wadia, J. S., and Dowdy, S. F. (2005) Cationic TAT peptide transduction domain enters cells by macropinocytosis (vol 102, pg 247, 2005). *J. Controlled Release 107*, 571−572.
(29) Thorén, P. E. G., Persson, D., Karlsson, M., and Nordén, B. (2000) The Antennapedia peptide penetratin translocates across lipid bilayers: The first direct observation. *FEBS Lett. 482*, 265−268.
(30) Persson, D., Thoren, P. E., Herner, M., Lincoln, P., and Norden, B. (2003) Application of a novel analysis to measure the binding of the membrane-translocating peptide penetratin to negatively charged liposomes. *Biochemistry 42*, 421−429.
(31) Yi, D. D., Li, G. M., Li, G., and Liang, W. (2007) Interaction of arginine oligomer with model membrane. *Biochem. Biophys. Res. Commun. 359*, 1024−1029.
(32) Herce, H. D., Garcia, A. E., Litt, J., Kane, R. S., Martin, P., Enrique, N., Rebolledo, A., and Milesi, V. (2009) Arginine-Rich Peptides Destabilize the Plasma Membrane, Consistent with a Pore Formation Translocation Mechanism of Cell-Penetrating Peptides. *Biophys. J. 97*, 1917−1925.
(33) Chan, D. I., Prenner, E. J., and Vogel, H. J. (2006) Tryptophan- and arginine-rich antimicrobial peptides: Structures and mechanisms of action. *Biochim. Biophys. Acta 1758*, 1184−1202.
(34) Zhang, X. A., Oglecka, K., Sandgren, S., Belting, M., Esbjörner, E. K., Nordén, B., and Gräslund, A. (2010) Dual functions of the human antimicrobial peptide LL-37: Target membrane perturbation and host cell cargo delivery. *Biochim. Biophys. Acta 1798*, 2201−2208.